Multi Material Topological Optimization of Structures and Mechanisms

Jonathan D. Hiller
Computational Synthesis Laboratory
Cornell University
Ithaca NY, 14853, USA
(607) 254-8940
jdh74@Cornell.edu

Hod Lipson
Computational Synthesis Laboratory
Cornell University
Ithaca NY, 14853, USA
(607) 255-1686
Hod.Lipson@Cornell.edu

ABSTRACT
Multi-material 3D-printing technologies permit the freeform fabrication of complex spatial arrangements of materials in arbitrary geometries. This technology has opened the door to a large mechanical design space with many novel yet non-intuitive possibilities. This space is not easily searched using conventional topological optimization methods such as homogenization. [1] Here we present an evolutionary design process for three-dimensional multi-material structures that explores this design space and designs substructures tailored for custom functionalities. The algorithm is demonstrated for the design of 3D non-uniform beams and 3D compliant actuators.

Categories and Subject Descriptors
J.6 [**Computer Applications**]: Computer-Aided Engineering – *Computer Aided Design.*

General Terms
Design, Experimentation

Keywords
Multi-material composites, Topological optimization, Shape optimization, Solid freeform fabrication

1. INTRODUCTION
In the engineering world, the method of fabrication dictates the mode of design. Traditional machine tools naturally create single material parts with straight lines, flat surfaces, and circular profiles. Thus, the current engineering design paradigm is feature-based modeling, in which two dimensional sketches are extruded, revolved, swept, and patterned to create three-dimensional parts of a single, homogenous material. With the advent of manufacturing techniques which easily create freeform (smooth) geometry and arbitrary internal material distributions, the constraints of the current computer aided design (CAD) paradigm become crippling. [2]

Permission to make digital or hard copies of all or part of this work for personal or classroom use is granted without fee provided that copies are not made or distributed for profit or commercial advantage and that copies bear this notice and the full citation on the first page. To copy otherwise, or republish, to post on servers or to redistribute to lists, requires prior specific permission and/or a fee.

GECCO'09, July 8–12, 2009, Montréal Québec, Canada.

Copyright 2009 ACM 978-1-60558-325-9/09/07...$5.00.

Additionally, despite the advent of powerful computing, human input is currently still crucial to transform a set of abstract functional goals into an instantiated design. A major challenge in automating the design process lies in the development of robust algorithms to address the spatial and physical constraints of a traditional feature-based manufacturing process, such as machining. [3] However, the advent of rapid prototyping and rapid manufacturing technology allows any 3D shape and topology to be fabricated without penalty, removing many complex constraints for the automated design process.

In this paper, we demonstrate the use of evolutionary algorithms to design the three dimensional material distribution of a cantilever beam to meet high-level functional goals not easily accomplished using current CAD tools. These goals include interdependent competing objectives that cannot be directly solved for. The solutions presented here are suitable for freeform fabrication, and uniquely take advantage of the capabilities of recent multi-material advances in 3D printing technology.

2. BACKGROUND

2.1 Freeform fabrication technologies
There are many fabrication technologies capable of creating smooth, freeform objects. Subtractive processes such as computer numerical controlled (CNC) milling selectively remove material from a homogenous block. Depending on the complexity of the machining system, overhangs and concave features may be possible, but internal cavities and complicated topologies often require prohibitive tooling and complexity. In contrast, additive manufacturing (3D printing, solid freeform fabrication) processes selectively build up a freeform object layer by layer, placing temporary supports where needed to create any geometry and topology. A variety of available commercial systems are capable of fabricating parts out of materials ranging from photoresins to stainless steel [4]. However, additive fabrication technology is largely limited to creating parts of a single, homogenous material.

The recent advent of multi-material freeform fabrication machines promises to exponentially expand the design-space for physical 3D parts. Currently, technology exists such that 3D objects can be seamlessly fabricated from two or more materials ranging from soft rubber to rigid polymers [5, 6]. These technologies allow complete freedom over the internal distribution of materials, including the ability to create repeating microstructures. However, CAD tools which can utilize these unique capabilities are lagging behind the fabrication technology itself.

2.2 Topology Optimization

The ideal design process would require the engineer to simply input the functional goals of the desired part, and would create the optimal blueprint autonomously. Much work has been done in this field [7, 8] regarding the topology or shape optimization of single material structures, with the goal of maximizing stiffness per weight. The most established method in this field is homogenization, as originally demonstrated by Bendsoe and Kikuchi. [1] This iterative process varies the effective stiffness of each cell within a 2D or 3D matrix according to its strain energy, and optimizes the structure subject to constraints on total volume and minimizing strain energy. Variations on this method have yielded results that maximize deflection, for applications such as a simple gripper structure, or even utilize two materials to emulate an actuated structure. [9-11]

However, homogenization results are generally limited to optimizing overall deflection or force. As complexity is added to the design problem, such as competing objectives involving multiple materials or specifying a desired deformed shape, homogenization approaches become unwieldy or even completely impractical.

Despite their generality, evolutionary algorithms have not found widespread use in topological optimization for several reasons. First, the homogenization method greatly outperforms genetic algorithms for the single objective structural optimization problems that are often addressed in literature. Secondly, the success of genetic algorithms depends strongly on the encoding (genotype) used to represent the physical object (phenotype). In early attempts at using genetic algorithms to solve topological optimization problems, every individual pixel or voxel was represented explicitly in the genotype [12, 13]. In addition to the challenge of making crossover and mutation non-destructive, this method scales poorly to large structures.

Thus, the success of genetic algorithms in solving topological optimization problems depends on using a representation that efficiently defines sensible objects using a minimum number of parameters [14]. Various graph structures, generative encodings, and constrained bit-wise encodings have been proposed to address these challenges, as summarized in Kicinger et al [15]. These more efficient representations enable genetic algorithms to overcome the functional complexity limitations of homogenization, although at the expense of increased computational effort.

3. METHODS

3.1 Encoding

Here we propose a pseudo-generative encoding which naturally generates smooth, freeform 2D and 3D shapes at an arbitrary level of complexity with a minimal number of parameters. The genotype consists of a series of frequency amplitudes at harmonic multiples, and the phenotype is generated by applying the inverse discrete fourier transform to this series. This representation was chosen for its relative simplicity of implementation and evolvability. By representing a three-dimensional object as a 3D matrix of frequency amplitude components, a number of advantages are realized. These include the ability to render the genotype at any resolution, complete dimensional independence, and naturally available symmetry.

There are a number of possible variations of the inverse discrete Fourier transform that could be utilized. Each implies a different set of boundary conditions. Each boundary within the domain can be even or odd at the left and right boundaries and symmetric about either its endpoint, or a point halfway to the adjacent point. This generates a total of 16 possibilities. Here we assume even, symmetric endpoint boundary conditions, which is commonly referred to as simply the discrete cosine transform (DCT).

Multidimensional fourier transforms such as the DCT also have the favorable property of linear independence. For instance, a 2D spatial object is constructed by applying the inverse DCT independently to each row, then to each column of a 2D matrix of frequency components. The result will be the same regardless of order. This extends into the 3rd dimension as well. The discrete cosine transform also compresses the most meaningful information about an arbitrary geometry into the lowest order frequency coefficients. For this reason, it is has been widely utilized in jpeg image compression. In 3D, this enables complex freeform (smooth) geometries to be represented with relatively few low-order coefficients.

The process of transforming the genotype into a phenotype is as follows:

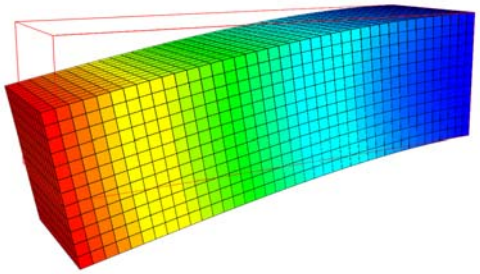
1. The dimensions of the geometrical envelope (workspace) are defined. Here, the physical evaluation is simulated in discrete voxel-space, and the dimensions of the cantilever beam are defined arbitrarily as 40×12×12 voxels (5760 total).
2. A complexity metric is defined to control the tradoff between level of detail and number of values in the genotype. Here, our complexity metric is arbitrarily chosen as 10, meaning that the longest dimension of the beam will have 10 frequency components. Scaling by the dimensions of the beam (40×12×12), the resulting frequency matrix will be 10×3×3 elements. We enforce symmetry along the Y axis, so only 1.5 (rounded up to 2) frequency components are necessary in this direction. This results in evolving only 60 values (10×2×3 frequency components) to represent a 5760 voxel structure, which makes this problem computationally feasible. The tradeoff is that sharp edges and flat surfaces are harder to evolve. Because the size ratio between the physical and frequency matrices is 4:1, features smaller than approximately 4 voxels are also more difficult to represent, and thus less likely to evolve.
3. The 3D matrix of frequency components is randomly initialized for each material present in the current experiment. These values range from -0.5 to 0.5 in dimensionless units. The range is arbitrary, and can be linearly scaled without effect.
4. If all components of the frequency matrix were randomly varying within the same interval, the higher order terms would dominate, and a randomly generated object would essentially just be high frequency 3D noise. Thus, before rendering the phenotype, the higher order coefficients of the frequency matrices are reduced by the square root of the 3D manhattan distance from the constant coefficient (zeroth order frequency) to

maintain a sensible overall structure with suitably complex topology.

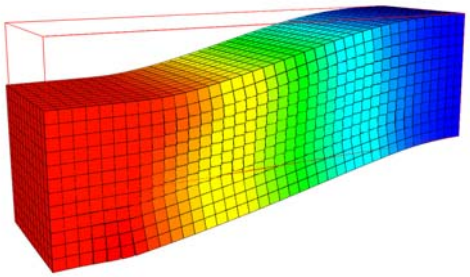
5. Before rendering the phenotype, each frequency matrix is padded with zeros to equal the dimension of voxels in the geometrical envelope.
6. The inverse DCT is applied sequentially for each material in each dimension. This results in a 3D density field for every material.
7. Each voxel within the geometrical envelope is instantiated as the material with the highest density at that location. In this case, we do not set a minimum density threshold, such that every voxel within the workspace is instantiated with one material.

3.2 Fitness Evaluation

The cantilever beam phenotypes were evaluated using the linear direct stiffness method, as illustrated in Figure 1. For each experiment, certain regions of voxels were defined as fixed to ground or subject to an applied force. Each material has an associated stiffness and poisson's ratio, which defines the global stiffness matrix for a given geometry. All six degrees of freedom were considered for each voxel, (3 translation, 3 rotational) resulting in a stiffness matrix with dimensionality of six times the number of voxels present. For these experiments, the stiffness matrix theoretically has approximately 1.2 billion elements, although fortunately it is very sparsely populated due to the limited local connectivity of the elements. This sparse stiffness matrix problem was then solved using the highly optimized PARDISO solver [16] to yield the resulting displacements of each voxel of the structure under load. Based on these displacements, internal stresses and reaction forces are then calculated in a post-processing step.



(a)



(b)

Figure 1: The direct stiffness method was used for physical evaluation of multi-material cantilever beams, here showing homogenous (a) and evolved (b) deformations

3.3 Algorithm Details

In the process of evolving objects using the DCT encoding, the following mutation and crossover operators were used:

3.3.1 Mutation

To mutate an individual, random variations were introduced into the frequency amplitudes of the genotype. These variations were kept small, such that any value could not change more than 10% for any given mutation. No bounds were placed on the range of values, allowing the algorithm to essentially re-scale all values instead of saturating at arbitrary limits. Recall that in our representation, low frequency components are weighted higher than the high frequency components. The mutation process preserves this general scaling, while allowing complete freedom for beneficial high frequency components to become more significant. For these experiments, 20% of the total frequency components are randomly selected for this variation with each mutation.

3.3.2 Crossover

When two individuals are selected for crossover, each frequency component of the offspring is randomly chosen from either parent. The parent which contributed the greatest number of frequency components is stored as the "most similar" parent for the selection process. In theory, this method of crossover works well as the algorithm converges on a specific topology. However, one challenge of the DCT encoding is that it is difficult for crossover to combine independent features of two children, since all frequency components affect the whole object to some degree.

3.3.3 Algorithm Parameters

For all experiments presented here, deterministic crowding selection was used. For our population size of 50 individuals, each individual was paired with a random mate and crossover was performed. If the child was more fit than its most similar parent, the child replaces the parent in the population. Otherwise, the offspring is disregarded. Table 1 summarizes the details of the genetic algorithm.

Table 1: Summary of experiment setup

Population Size	50
Selection method	Deterministic crowding
P(Mutation)	0.2
Solution Encoding	DCT generative

3.4 Algorithm Optimization

As in most evolutionary algorithms, the evaluation step is the most computationally expensive. Reasonable effort was made to optimize the code. It was written in C++ for low computational overhead, and the optimized PARDISO solver library was used for the heavy matrix calculations. This combination made the evolution of 40×12×12 voxel structures with approximately 35,000 degrees of freedom computationally feasible on a single desktop computer. Each evaluation takes less than four seconds on a single processor, dual core desktop computer at 3.2 GHz.

The resolution independence of the DCT encoding was also exploited to speed up the evolution process. First, an entire population was evolved using a domain of ½ the dimensions

(12.5% of the total voxels) by simply sampling the inverse fourier transform at half the density. These evaluate in a fraction of a second, resulting in an order of magnitude increase in speed over the full resolution evaluation. Once fitness begins to level off (less than 10% increase in the last half of the evaluations), the evaluation is switch to full resolution. (Figure 2) Fitness is usually reduced directly after the transition, but quickly recovers and continues to progress.

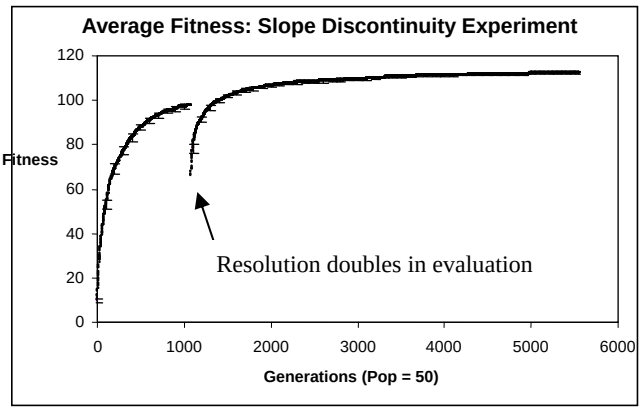
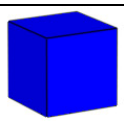
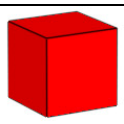
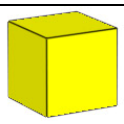


Figure 2: A representative fitness plot illustrates the effect of evolving with a low resolution phenotype before switching to a higher resolution population. The temporary drop in fitness upon switching resolution is quickly recovered.

4. RESULTS

Two different cases were chosen to illustrate the use of genetic algorithms in designing composite structures with high-level functionality. First, we considered the deflected shape of the top surface of a cantilever beam composed of stiff and flexible materials. A third, lighter material was then introduced along with an additional objective of minimizing structural weight. Secondly, we considered an actuator that maximizes the two-dimensional deflection of a beam tip subject to applied forces in the mutually orthogonal direction to the desired deflection. The two material single objective configuration and the three material multi-objective configurations were both considered in this case as well. The physical parameters of the materials used in all these experiments are outlined in Table 2. These material properties are similar to those which can be printed with existing multi-material freeform fabrication processes.

Table 2: Summary of experimental materials

Color	Blue (Stiff)	Red (Flexible)	Yellow (Lightweight)
Element Shape			
Stiffness	15 MPa *	0.15 MPa	1.5 MPa
Poisson's ratio	0.3	0.3	0.3
Density	1.2 g/cm3	1.2 g/cm3	0.12 g/cm3

*Several experiments use 150MPa, as noted in text

4.1 Deflected beam shapes

4.1.1 Single objective optimization

Given a cantilever beam, a variety of desired deflected shapes were selected, departing to varying degrees from the normal third-order polynomial profile. In order to observe interesting behavior, two materials of varying stiffness were considered in a domain of 40×12×12mm. Each voxel was a 1mm cube, and symmetry along the vertical plane parallel to the major axis of the beam was enforced. The resulting geometries are shown in Figure 3, along with plots showing the deflected shape, the desired deflected shape, and the deflection of a nominal, homogenous single material beam. The deviation of the actual beam from the desired profile is also plotted, along with the RMS error between the two.

A straight profile was considered as a simple geometry which ideally needs only a single region of each material for the ideal solution. The result (Figure 3a) shows the expected distribution of flexible material near the grounded edge and stiff material composing the rest of the beam. Deviation from the nominal profile was very low, at three orders of magnitude less than the dimension of a single voxel.

A circular (arc) deflected profile was also considered. (Figure 3b) The solution to this is somewhat more complex than for the simple straight line but just as effective, with very low deviation from the desired shape.

To explore the ability of the evolutionary algorithm to find solutions in non-obvious sub-domains, a quadratic profile with negative (upward) curvature was defined. Here, the resulting beam does in fact exhibit negative curvature, which requires a fundamentally different solution than for positive curvature beams. (Figure 3c) However, the solution did not match the profile of the beam well, likely because it is not possible to match the non-zero slope at the fixed boundary condition. However, upon defining a 4^{th} order polynomial profile involving both positive and negative curvature that matches the fixed zero slope boundary condition of the cantilever beam, the result improves remarkably. (Figure 3d) There is a small deviation at the free end, but this is likely because it is physically impossible to perfectly match a zero-slope boundary condition at the end of deflected cantilever beam. A stiffness ratio of 1000:1 between the stiff and flexible materials was used in this case to enable a wider variety of solutions.

We also considered two cases of discontinuity in the desired profiles. In the first case, a discontinuous slope was applied by combining two linear functions piece-wise. (Figure 3e) The algorithm returned a favorable result, with the largest deviations occurring right around the discontinuity, as expected. This was still well bounded at two orders of magnitude less than the dimension of a voxel. Finally, to test the limits of the algorithm to fit a function, a discontinuous step function was considered. (Figure 3f) Even with a 1000:1 material stiffness ratio, the results are similar to those observed with the negative curvature quadratic case, which is to say that very large errors were observed around the area of discontinuity.

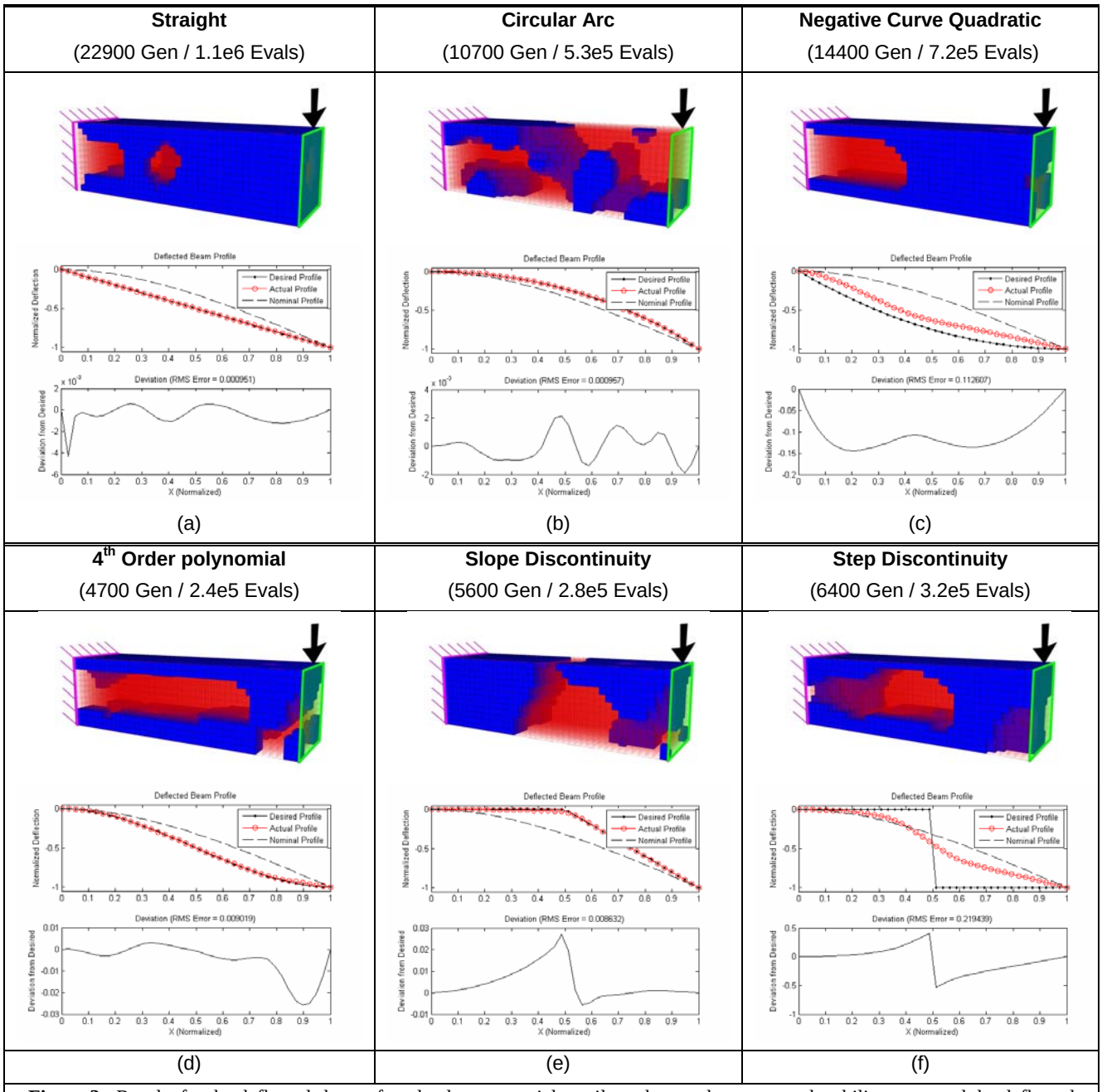


Figure 3: Results for the deflected shape of evolved two material cantilever beams demonstrate the ability to control the deflected profile of the beam to a high degree of accuracy, including slope discontinuities and upward curvatures. Blue material is a factor of 100 or 1000 times stiffer than the red (shown translucent) material.

4.1.2 Multi objective optimization

An additional criterion of minimizing weight was introduced to add complexity to the optimization problem. The stiff and flexible materials explored in the previous experiments were preserved, and interpreted to be of equal density. A third, much lighter material was introduced, with an intermediate stiffness. This creates a situation where the ideal solution will very likely make use of all three materials. The fitness used in the previous experiments was rewarded by up to 50% of its value according to the total mass of the beam. Results of this multi-objective optimization are shown in Figure 4.

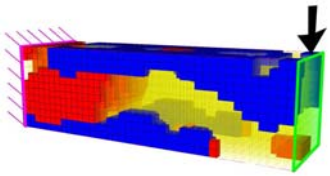
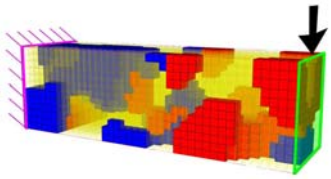
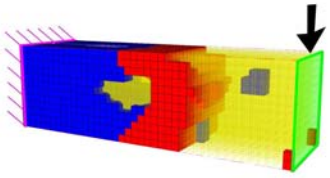
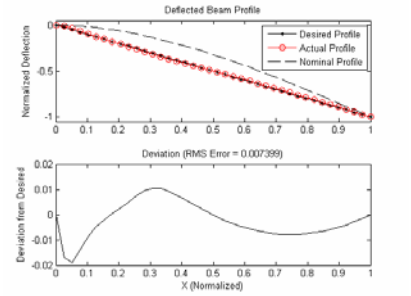
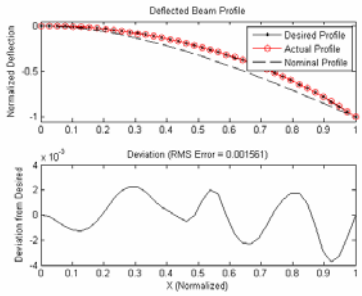
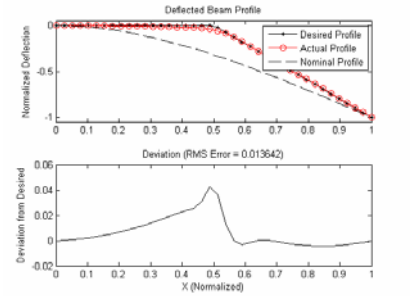
Straight (15000 Gen / 7.5e5 Evals)	**Circular Arc** (14300 Gen / 7.1e5 Evals)	**Slope Discontinuity** (13500 Gen / 6.7e5 Evals)
Normalized Weight: **0.556**	Normalized Weight: **0.447**	Normalized Weight: **0.502**
		
		

Figure 4: Results for the deflected shapes of three material beams are similar to the two material results, while additionally optimizing for the lightest structure. The low density material (yellow, shown translucent) has an intermediate stiffness between the stiff blue and flexible red materials

Three of the desired profiles from the single objective experiments were selected for multi-objective optimization. The linear deflection case (Figure 4a) resulted in a slightly worse fit than the single objective case, but based on the properties of the materials presented in Table 2, has a density of nearly half that of the two material solution. The circular arc case (Figure 4) was only a factor of two worse in matching the desired profile, and yet was less than half the density of the single objective case. Finally, in the case of the discontinuous slope, the profile fit metric was only slightly worse, while the resulting beam was almost half the density.

4.2 Two-Force actuator

The optimization of a planar actuator was also considered. The loading conditions are shown in Figure 5. Two input forces are applied midway down the beam parallel to the major axis of the beam. These forces range from -0.1 to 0.1 newtons, and the output is the displacement of the tip of the beam in the two orthogonal directions to the major axis of the beam. Fitness was defined as the reachable area of the center of the tip of the beam. The domain of these problems was constrained to 20×6×6mm, with 1mm cubic voxels. No symmetry constraints were imposed in order to allow greater design space of the solutions. In a manner similar to the previous experiments, an additional objective of minimizing weight was also considered. The resulting geometry and tip tracing areas are shown in Figure 6 for the single objective (two material) and multi objective (three material) cases.

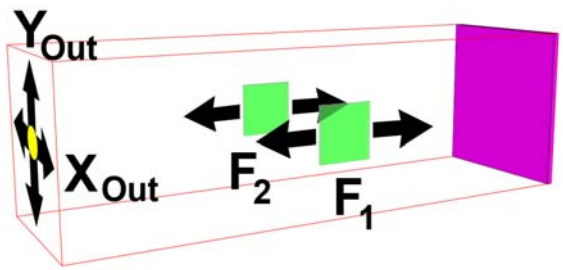


Figure 5: The loading conditions for the actuator optimization present a high-level, non-intuitive problem

In both solutions, the algorithm came up with very similar solutions that make intuitive sense upon examination. A single row of stiff material connects the grounded face of the beam to the mid-plane of the beam where the forces are applied, while the rest of the beam is filled in with the most flexible material. Regions of stiff material (or the lighter, semi-stiff material) connect this strand to the two locations of applied force. The outer half of the beam essentially has no forces acting on it. Thus, in the single objective case, this region was effectively ignored, leading to a mostly random material distribution within it. However, the addition of the density objective provided incentive for this unused area to become strictly light material, which accounts for nearly all the difference in the density of the three-material beam, which is approximately 60% of the mass of the two-material beam.

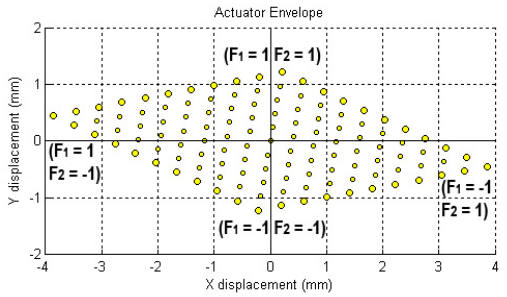
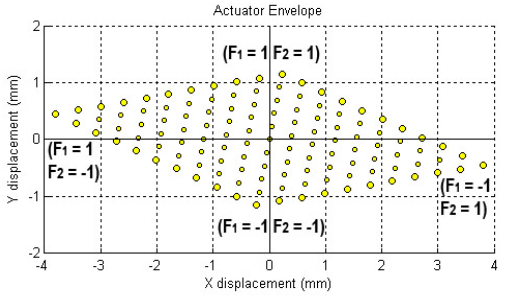
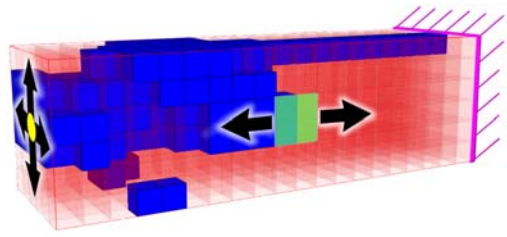
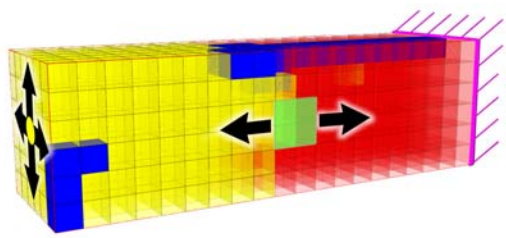
Single Objective (5000 Gen / 2.5e5 Evals)	**Multi-Objective** (19500 Gen / 9.8e5 Evals)
Two Materials (Normalized Density = **1.0**)	Three materials (Normalized Density = **0.604**)
	
	

Figure 6: Evolved beam actuators are shown that maximize the potential swept area of the tip of the beam. Both single objective and multi-objective weight-optimized results show very similar topology and behavior.

The resulting tip-deflection plots for the two are extremely similar, although the two-material solution is approximately 0.6% better. This demonstrates the ability of the algorithm to repeatably solve a given high-level structural problem in a similar optimal manner, even under varying objective pressures.

In general, the results presented here have been left to run for several thousand generations, with a population size of 50 for a total of several hundred thousand evaluations. This corresponds roughly to running on a quad core CPU overnight. It should be noted that good results were obtained with a much lower number of evaluations, but the best results (after running overnight or longer) are presented here.

5. CONCLUSIONS

Genetic algorithms are suitable for designing the complex multi-material objects that have recently become possible to fabricate using additive manufacturing techniques. The lack of existing software design tools to fully take advantage of the capabilities of these fabrication processes enables genetic algorithms to fill a new niche in the mechanical design space. Instead of designing an object using existing CAD programs or other traditional means, genetic algorithms allow the engineer to simply set high-level goals to be fulfilled.

We have demonstrated this using two very different mechanical criteria of simple cantilever beams. By specifying the desired deflected shape of a beam, or defining vague goals of maximizing deflection area of a compliant actuator, we create a problem that cannot be easily solved using current state-of-the-art topological optimization tools such as homogenization. Additionally, by introducing multiple objectives, for example minimizing weight in addition meeting the previous criteria, we demonstrated the flexibility of genetic algorithms to easily adapt to competing objectives of very different problems. These results open the door to robust, high-level design tools that are easily adapted to more complex design problems to fully utilize the capabilities of multi-material additive fabrication techniques.

6. ACKNOWLEDGMENTS

This work was supported in part by a National Science Foundation Graduate Research Fellowship and NSF Creative-IT grant 0757478.

7. REFERENCES

[1] Bendsoe, M. P. and Kikuchi, N. "Generating optimal topologies in structural design using a homogenization method." *Comput. Methods Appl. Mech. Eng.*, Vol. 71, 1988, pp. 197-224.

[2] Hague, R., Campbell, I. and Dickens, P. "Implications on design of rapid manufacturing." *Proceedings of the Institution of Mechanical Engineers, Part C: Journal of Mechanical Engineering Science*, Vol. 217, 2003, pp. 25-30.

[3] Mantyla, M., Nau, D. and Shah, J. "Challenges in feature-based manufacturing research." *Commun. ACM*, Vol. 39, 1996, pp. 77-85.

[4] Beaman, J. J., Marcus, H. L., Bourell, D. L., Barlow, J. W., Crawford, R. H. and McAlea, K. P. *Solid Freeform Fabrication: A New Direction in Manufacturing*. Kluwer Academic Publishers, 1997.

[5] Malone, E., Rasa, K., Cohen, D., Isaacson, T., Lashley, H. and Lipson, H. "Freeform fabrication of zinc-air batteries and electromechanical assemblies." *Rapid Prototyping Journal*, Vol. 10, 2004, pp. 58-69.
[6] Objet Geometries inc, http://www.objet.com (Accessed: January 28, 2009)
[7] Díaz, A. and Lipton, R. "Optimal material layout for 3D elastic structures." *Structural and Multidisciplinary Optimization*, Vol. 13, 1997, pp. 60-64.
[8] Fernandes, P., Guedes, J. M. and Rodrigues, H. "Topology optimization of three-dimensional linear elastic structures with a constraint on "perimeter"." *Computers & Structures*, Vol. 73, 1999, pp. 583-594.
[9] Buehler, M. J., Bettig, B. and Parker, G. G. "Topology Optimization of Smart Structures Using a Homogenization Approach." *Journal of Intelligent Material Systems and Structures*, Vol. 15, 2004, pp. 655-667.
[10] Nishiwaki, S., Frecker, M. I., Min, S. and Kikuchi, N. "Topology optimization of compliant mechanisms using the homogenization method." *International Journal for Numerical Methods in Engineering*, Vol. 42, 1998, pp. 535-559.
[11] Sigmund, O. and Torquato, S. "Design of smart composite materials using topology optimization." *Smart Materials and Structures*, Vol. 8, 1999, pp. 365-379.
[12] Jakiela, M. J., Chapman, C., Duda, J., Adewuya, A. and Saitou, K. "Continuum structural topology design with genetic algorithms." *Computer Methods in Applied Mechanics and Engineering*, Vol. 186, 2000, pp. 339-356.
[13] Kane, C. "Topological Optimum Design using Genetic Algorithms." *Control and Cybernetics*, Vol. 25, 1996, pp. 1059--1088.
[14] Kane, C. and Schoenauer, M. *Genetic operators for two-dimentional shape optimization.* City, 1996.
[15] Kicinger, R., Arciszewski, T. and Jong, K. D. "Evolutionary computation and structural design: A survey of the state-of-the-art." *Computers & Structures*, Vol. 83, 2005, pp. 1943-1978.
[16] PARDISO Solver Project, http://www.pardiso-project.org (Accessed: January 28, 2009)